Electronic Supplementary Information for

Constructing highly efficient multiple-resonance fluorescence materials through inserting benzothiophene within B/N skeletons

He Zhao, [a] Wenkun Han,*[b] Jianan Xu, [b] Yan Bi, [b] He Li, [b] Tianyu Yang, [b] Xiaoyu Ma, *[b] and Chunhui Su,*[a]

[a] *School of Materials Science and Engineering, Changchun University of Science and Technology, Changchun, P.R. China. E-mail: sch@cust.edu.cn.*

[b] *Research and Development Department, Jilin OLED Material Tech Co., Ltd, Changchun, P.R. China. E-mail: maxy@jl-oled.com; wenkunhan@outlook.com.*

Experimental

General information

All chemical compounds were commercially available. Reaction reagents were purchased from Energy Chemical Co. and/or J&K Scientific Ltd. Co. and immediately used without further purification. The ^{1}H nuclear magnetic resonance (^{1}H NMR) spectra were measured on Avance-400 (Bruker, 400 MHz) spectrometer. Chloroform-d ($CDCl_3$) was used for ^{1}H NMR analysis. Ultraviolet−visible (UV−vis) absorption spectra were recorded on a Hitachi U-3900 spectrophotometer. Fluorescence spectra were determined by a Horiba FluoroMax-4 spectrophotometer. Differential scanning calorimetry (DSC) characteristics were detected by a NETZSCH DSC204 instrument following the heating rate of 10 °C/min between 50 and 500 °C under a nitrogen atmosphere, and thermogravimetric analysis (TGA) were determined using a TA Q600 thermogravimeter at a heating rate of 10 °C/min between 50 and 800 °C under nitrogen conditions to monitor weight loss. The HOMO levels were estimated using a cyclic voltammetry (Ivium Tech., Iviumstat). Cyclic voltammetry (CV) curves of samples were investigated by a BAS 100W Bioanalytical electrochemical work station using platinum disk as working electrode, platinum wire as auxiliary electrode, a porous glass wick Ag/Ag^+ as pseudo reference electrode and ferrocene/ferrocenium (Fc/Fc^+) as the internal standard. The redox potential was recorded at a scan rate of 100 mV s^{-1} in a 0.1 M solution and tetrabutylammonium hexafluorophosphate ($TBAPF_6$) was as the electrolyte. The mass spectra were performed using a JMS-700 (JEOL) with high resolution fast atom bombardment

(FAB) mode and Advion Expression-L CMS spectrometer in APCI mode. The photoluminescence quantum yields (PLQYs) were tested using the Yokohama C9920-02G assay system.

Single-crystal X-ray diffraction: Single crystal X-ray diffraction data were collected on a Rigaku Synergy-DS diffractometer with Mo KR and Control Software, using the RAPID AUTO at 293 K. The structures were solved with direct methods and refined with a full-matrix least-squares technique, using the Olex2 programs, respectively. The crystallographic data has been deposited with Cambridge Crystallographic Data Centre (CCDC), and signed to CCDC code 2348531 for SBN-1, 2348530 for SBN-2, respectively.

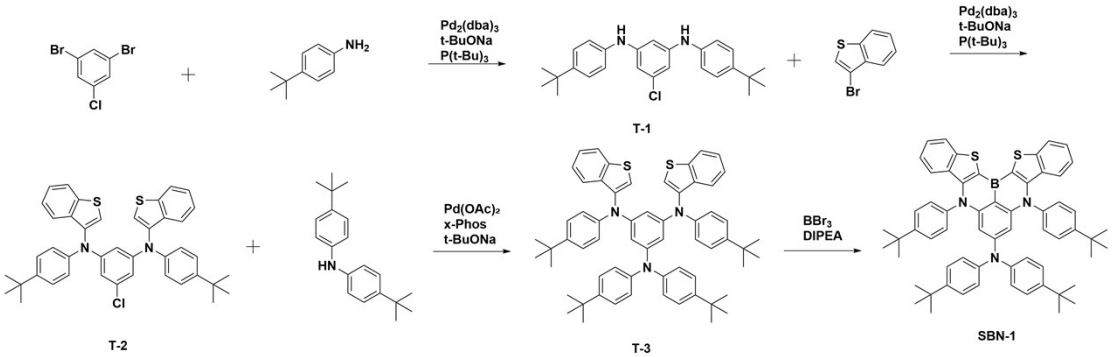

Scheme S1. Synthesis scheme of **SBN-1**.

N1,N3-bis(4-(tert-butyl)phenyl)-5-chlorobenzene-1,3-diamine（T-1）

1,3-dibromo-5-chlorobenzene (4.00 g, 14.80 mmol), 4-(tert-butyl)aniline (4.60 g, 31.00 mmol), $Pd_2(dppa)_3$ (0.27 g, 0.30 mmol), t-BuONa (3.13 g, 32.60 mmol), P(t-Bu)$_3$ (0.06 g, 0.30 mmol) were dissolved in toluene (225 mL) under a nitrogen atmosphere. After stirring at room temperature for 6 h, the reaction mixture was added 200 ml water to quench the reaction, and washed with water (300 mL, three times), and collected the organic phase, then dried over magnesium sulfate. After the solvent was removed in vacuo, the crude product was purified by silica gel column chromatography (eluent: petroleum ether/dichloromethane = 4/1) to obtain white compound (5.40 g, yield: 91%). ^{1}H NMR (400 MHz, Chloroform-d) δ 7.34 – 7.26 (4 H, m), 7.07 – 6.99 (4 H, m), 6.49 (3 H, dd, J 12.7, 2.0), 5.72 (2 H, s), 1.31 (18 H, s). ^{13}C NMR (101 MHz, Chloroform-d) δ 146.10, 145.44, 139.05, 135.72, 126.23, 119.77,

108.08, 102.01, 34.28, 31.45. HRMS (EI/MS) m/z $[M]^+$ calcd for $C_{26}H_{31}ClN_2$: 406.9980; observed: 407.2249.

N1,N3-bis(benzo[b]thiophen-3-yl)-N1,N3-bis(4-(tert-butyl)phenyl)-5-chlorobenzene-1,3-diamine (T-2)

T-1 (5.00 g, 12.3 mmol), 3-bromobenzo[b]thiophene (5.3 g, 25.00 mmol), $Pd_2(dppa)_3$ (0.23 g, 0.25 mmol), t-BuONa (2.25 g, 25.00 mmol), $P(t\text{-}Bu)_3$ (0.50 g, 0.25 mmol) were degassed and purged with N_2 for three times. Toluene (230 mL) was added into the reaction via syringe. After heating the reaction mixture at 100 °C for 12 h. After the reaction mixture cool down to room temperature, 200 mL water were added. Then, collected the organic phase and dried over anhydrous $MgSO_4$. After evaporation, the crude product was purified by silica gel column using dichloromethane/petroleum ether (1:4, v/v) as eluant, and then the resulting white solid was obtained (7.02 g, yield: 85%). ^{1}H NMR (400 MHz, Chloroform-d) δ 1.23 – 1.28 (18 H, s), 6.32 – 6.38 (1 H, t, J 2.1), 6.47 – 6.52 (2 H, d, J 2.1), 6.85 – 6.94 (4 H, m), 6.98 – 7.02 (2 H, s), 7.04 – 7.12 (4 H, m), 7.21 – 7.30 (2 H, m), 7.31 – 7.41 (4 H, m), 7.76 – 7.83 (2 H, d, J 8.0). ^{13}C NMR (101 MHz, Chloroform-d) δ 148.96, 146.20, 143.63, 139.20, 139.13, 135.29, 135.01, 125.90, 124.64, 124.12, 123.13, 122.72, 122.56, 120.71, 112.83, 110.40, 34.25, 31.38. HRMS (EI/MS) m/z $[M]^+$ calcd for $C_{42}H_{39}ClN_2S_2$: 671.3580; observed: 671.2325.

N1,N3-bis(benzo[b]thiophen-3-yl)-N1,N3,N5,N5-tetrakis(4-(tert-butyl)phenyl)benzene-1,3,5-triamine (T-3)

T-2 (5.80 g, 8.65 mM), bis(4-(tert-butyl)phenyl)amine (2.45 g, 8.70 mmol), $Pd(OAc)_2$ (0.015 g, 0.09 mmol), X-Phos (0.043 g, 0.09 mmol), t-BuONa (1.67 g, 17.4 mmol) were degassed and purged with N_2 for three times. After adding xylenes (200 mL), the mixture was stirred at 160 °C for 10 h. Then cool down the reaction to room temperature, 200 mL water was added into the mixture. Collected the organic phase and dried over anhydrous $MgSO_4$. Then the organic solvent was removed with a rotary evaporator, and the resulting precipitate was purified by silica gel column using dichloromethane/petroleum ether (1:4, v/v) as eluant, and then the resulting white solid was obtained (6.5 g, yield: 82%). ^{1}H NMR (400 MHz, Chloroform-d) δ 7.80 –

7.73 (1 H, dt, J = 0.9, 8.0 Hz), 7.43 – 7.32 (2H, m), 7.32 – 7.24 (1H, ddd, J = 1.1, 7.0, 8.0 Hz), 7.11 – 7.02 (2H, m), 7.01 – 6.94 (2H, m), 6.94 – 6.85 (3H, m), 6.83 – 6.74 (2H, m), 6.28 – 6.24 (2H, s), 1.33 – 1.20 (18H, d, J = 2.6 Hz). ^{13}C NMR (101 MHz, Chloroform-d) δ 149.03, 148.05, 145.17, 144.74, 144.65, 144.33, 139.98, 139.08, 135.50, 125.55, 125.51, 124.34, 123.78, 123.52, 122.98, 122.89, 121.35, 119.14, 110.64, 109.22, 34.11, 31.39. HRMS (EI/MS) m/z $[M]^+$ calcd for $C_{62}H_{65}N_3S_2$: 916.3430; observed: 916.4691.

N,N,5,9-tetrakis(4-(tert-butyl)phenyl)-5H,9H-14,15-dithia-5,9-diaza-14b-boradiindeno[2,1-a:1',2'-j]phenalen-7-amine (SBN-1)

T-3 (6.50 g, 7.10 mmol) was degassed and purged with N_2 three times and then 150 mL 1,2-dichlorobenzene (o-DCB) was added. BBr_3 (3.50 g, 14.00 mmol) was added dropwise into the mixture with stirring at 0 °C in ice-water. After the reaction mixture was stirring at room temperature for 4 h, the reaction mixture was allowed to cool to 0 °C DIPEA (2.70 g, 21.00 mmol) was added into the reaction mixture，and then the reaction mixture was further stirred at 120 ºC for 12 h. After cooling to room temperature, the reaction mixture was carefully quenched by addition of water. The product was extracted with dichloromethane, and the combined organic layer was dried over anhydrous $MgSO_4$. After filtration and evaporation, and the resulting precipitate was purified by silica gel column using dichloromethane/petroleum ether (1:4, v/v) as eluant, and then the resulting yellow-green solid was obtained (4.20 g, yield: 65%). ^{1}H NMR (400 MHz, Chloroform-*d*) δ 7.93 (2 H, d, J 8.0), 7.49 (4 H, d, J 8.0), 7.31 – 7.22 (8 H, m), 7.14 – 7.07 (4 H, m), 6.90 – 6.83 (6 H, m), 5.89 (2 H, d, J 8.6), 1.37 (18 H, s), 1.28 (18 H, s). ^{13}C NMR (101 MHz, Chloroform-d) δ 152.39, 150.40, 148.26, 145.49, 144.58, 144.49, 143.69, 139.93, 132.41, 129.77, 127.28, 125.42, 124.96, 124.52, 123.95, 123.37, 122.85, 100.82, 34.87, 34.21, 31.51, 31.47. HRMS (EI/MS) m/z $[M]^+$ calcd for $C_{62}H_{62}BN_3S_2$: 924.1290; observed: 923.4476.

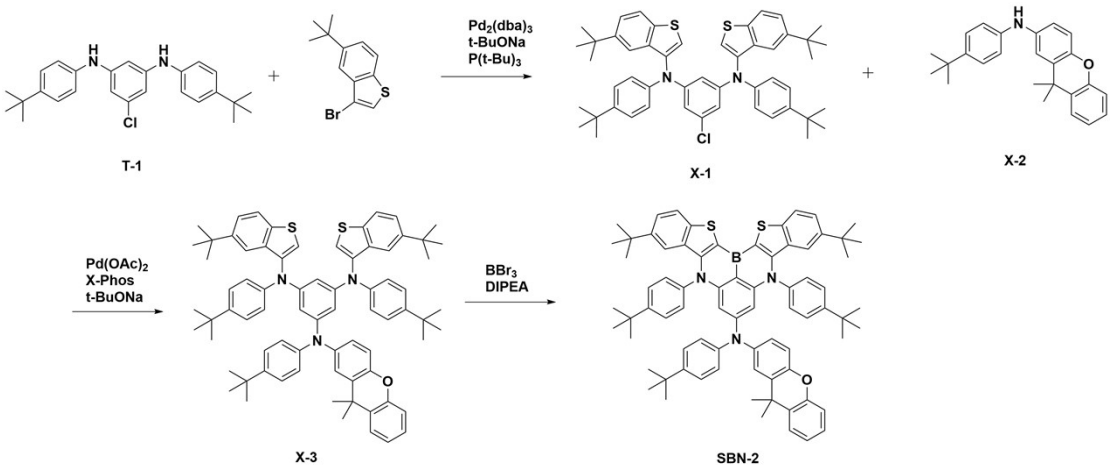

Scheme S2. Synthesis scheme of **SBN-2**.

N1,N3-bis(5-(tert-butyl)benzo[b]thiophen-3-yl)-N1,N3-bis(4-(tert-butyl)phenyl)-5-chlorobenzene-1,3-diamine (X-1)

T-1 (5.00 g, 12.3 mmol), 3-bromo-5-(tert-butyl)benzo[b]thiophene (6.73 g, 25.00 mmol), $Pd_2(dppa)_3$ (0.23 g, 0.25 mmol), t-BuONa (2.25 g, 25.00 mmol), $P(t\text{-}Bu)_3$ (0.50 g, 0.25 mmol) were degassed and purged with N_2 for three times. Toluene (240 mL) was added into the reaction via syringe. After heating the reaction mixture at 100 °C for 12 h. After the reaction mixture cool down to room temperature, 200 mL water were added. Then, collected the organic phase and dried over anhydrous $MgSO_4$. After evaporation, the crude product was purified by silica gel column using dichloromethane/petroleum ether (1:4, v/v) as eluant, and then the resulting white solid was obtained (8.86 g, yield: 79%). ^{1}H NMR (400 MHz, Chloroform-*d*) δ 7.74 – 7.66 (2 H, m), 7.40 (2 H, dt, J 8.4, 2.4), 7.23 (1 H, d, J 3.7), 7.11 (4 H, td, J 6.0, 5.6, 2.6), 6.92 (5 H, dq, J 8.0, 2.7), 6.63 – 6.52 (3 H, m), 1.30 – 1.17 (36 H, m). ^{13}C NMR (101 MHz, Chloroform-d) δ 149.08, 147.09, 146.15, 143.59, 139.24, 136.46, 135.02, 134.95, 125.89, 122.89, 122.81, 122.53, 119.13, 119.02, 113.59, 111.70, 34.64, 34.27, 31.44, 31.39. HRMS (EI/MS) m/z $[M]^+$ calcd for $C_{42}H_{39}ClN_2S_2$: 783.5740; observed: 783.3567.

N-(4-(tert-butyl)phenyl)-9,9-dimethyl-9H-xanthen-3-amine (X-2)

^{1}H NMR (400 MHz, Chloroform-*d*) δ 7.68 (2 H, d, J 8.5), 7.42 (2 H, dt, J 1.5, 8.5), 7.34 (3 H, hept, J 1.3), 7.17 (1 H, ddd, J 1.6, 7.3, 8.9), 7.10 (1 H, q, J 1.4), 6.97 – 7.08

(6 H, m), 6.83 – 6.97 (8 H, m), 6.78 (2 H, t, J 1.3), 6.67 – 6.74 (2 H, m), 6.35 (3 H, s), 1.41 – 1.46 (6 H, m), 1.22 (27 H, dd, J 1.1, 5.8), 1.29 (18 H, s). ^{13}C NMR (101 MHz, CDCl3) δ 150.61, 145.52, 143.09, 141.92, 138.20, 130.82, 129.63, 127.33, 126.12, 122.82, 119.14, 116.98, 116.29, 34.21, 34.09, 32.31, 31.49, 29.71. HRMS (EI/MS) m/z $[M]^+$ calcd for $C_{25}H_{27}NO$: 357.2093; observed: 358.2167.

N1,N3-bis(5-(tert-butyl)benzo[b]thiophen-3-yl)-N1,N3,N5-tris(4-(tert-butyl)phenyl)-N5-(9,9-dimethyl-9H-xanthen-2-yl)benzene-1,3,5-triamine (X-3)

In a 250 mL round flask, X-1(6.12 g, 7.81 mmol), X-2 (2.79 g, 7.81 mmol), $Pd(OAc)_2$ (0.013 g, 0.0781 mmol), X-Phos (0.035 g, 0.0781 mmol), t-BuONa (0.76 g, 7.9 mmol) were degassed and purged with N_2 for three times. After adding xylenes (200 mL), the mixture was stirred at 160 °C overnight. Then cool down the reaction to room temperature, 200 mL water was added into the mixture. Collected the organic phase and dried over anhydrous $MgSO_4$. Then the organic solvent was removed with a rotary evaporator, and the resulting precipitate was purified by silica gel column using dichloromethane/petroleum ether (1:4, v/v) as eluant, and then the resulting white solid was obtained (7.07 g, yield: 82%). ^{1}H NMR (400 MHz, Chloroform-*d*) δ 7.68 (2 H, d, J 8.5), 7.42 (2 H, dt, J 8.5, 1.5), 7.34 (3 H, hept, J 1.3), 7.17 (1 H, ddd, J 8.9, 7.3, 1.6), 7.10 (1 H, q, J 1.4), 7.08 – 6.97 (6 H, m), 6.97 – 6.83 (8 H, m), 6.78 (2 H, t, J 1.3), 6.74 – 6.67 (2 H, m), 6.35 (3 H, s), 1.46 – 1.41 (6 H, m), 1.29 (18 H, s), 1.22 (27 H, dd, J 5.8, 1.1). ^{13}C NMR (101 MHz, Chloroform-d) δ 150.52, 149.11, 148.36, 146.74, 146.53, 144.88, 144.75, 144.61, 144.27, 142.19, 140.04, 136.45, 135.20, 130.61, 129.76, 127.28, 126.04, 125.52, 125.41, 124.94, 123.15, 122.89, 122.60, 122.48, 121.81, 121.65, 119.32, 118.00, 116.91, 116.29, 111.05, 110.13, 34.69, 34.11, 34.06, 32.22, 31.57, 31.38, 29.73, 14.15. HRMS (EI/MS) m/z $[M]^+$ calcd for $C_{75}H_{81}N_3OS_2$: 1104.6130; observed: 1104.5895.

3,11-di-tert-butyl-N,5,9-tris(4-(tert-butyl)phenyl)-N-(9,9-dimethyl-9H-xanthen-2-yl)-5H,9H-14,15-dithia-5,9-diaza-14b-boradiindeno[2,1-a:1',2'-j]phenalen-7-amine (SBN-2) H (400 MHz, Chloroform-d) 1.22 (27 H, dd, J 1.1, 5.8), 1.29 (18 H, s), 1.41 – 1.46 (6 H, m), 6.35 (3 H, s), 6.67 – 6.74 (2 H, m), 6.78 (2 H, t, J 1.3), 6.83 –

6.97 (8 H, m), 6.97 – 7.08 (6 H, m), 7.10 (1 H, q, J 1.4), 7.17 (1 H, ddd, J 1.6, 7.3, 8.9), 7.34 (3 H, hept, J 1.3), 7.42 (2 H, dt, J 1.5, 8.5), 7.68 (2 H, d, J 8.5).

X-3 (6.20 g, 5.62 mmol) was degassed and purged with N_2 three times and then 150 mL 1,2-dichlorobenzene (o-DCB) was added. BBr_3 (2.81 g, 11.24 mmol) was added dropwise into the mixture with stirring at 0 °C in ice-water. The reaction mixture was stirred at room temperature for 3 h. Then, DIPEA was added into the reaction mixture under 0 °C, and then the reaction mixture was further stirred at 120 ºC for 12 h. After cooling to room temperature, the reaction mixture was carefully quenched by addition of water. Collect organic solvent and dry by $MgSO_4$, and then the solvent was evaporated. The residue was purified by silica gel column using dichloromethane/petroleum ether (1:4, v/v) as eluant, and then the resulting yellow-green solid was obtained (2.84 g, yield: 46%). ^{1}H NMR (400 MHz, Chloroform-d) δ 7.84 (2 H, d, J 8.5), 7.46 (4 H, d, J 8.3), 7.40 – 7.28 (8 H, m), 7.21 (1 H, ddd, J 8.4, 7.3, 1.6), 7.12 – 6.99 (6 H, m), 6.92 – 6.84 (2 H, m), 6.81 – 6.70 (2 H, m), 6.42 (2 H, s), 1.51 (6 H, s), 1.27 (27 H, d, J 5.2), 1.03 (18 H, s). ^{13}C NMR (101 MHz, Chloroform-d) δ 152.05, 150.42, 148.60, 146.90, 145.54, 144.96, 144.32, 143.10, 142.45, 141.78, 139.87, 132.38, 130.80, 129.82, 129.67, 127.43, 127.34, 126.26, 126.03, 125.51, 125.23, 124.91, 123.14, 123.03, 122.82, 122.64, 121.66, 119.81, 116.83, 116.42, 113.97, 99.13, 34.74, 34.61, 34.16, 34.09, 32.40, 31.49, 31.32. HRMS (EI/MS) m/z $[M]^+$ calcd for $C_{75}H_{78}BN_3OS_2$: 1112.3990; observed: 1112.5709.

Theoretical calculation

The calculations were performed using the Gaussian 16 package based on the density functional theory (DFT) and time-dependent density functional theory (TD-DFT) methods with the b3lyp hybrid functional. All structures were optimized using DFT (S_0 states) or TD-DFT (S_1 states) method with a 6-31G(d,p) basis set. Franck-Condon analyses of emission spectra were performed according to the literature.[1] All calculations were performed in the gas phase. The first excited state showed local excitation mainly contributed by the HOMO orbital to the LUMO orbital.

The resonance effect of nitrogen atoms localizes HOMO on the carbons at their *ortho* and *para* positions, potentially undergoing electrophilic borylation. The introduction

of aromatic amino groups of central benzene rings fully promoted the desired borylation at the *para* carbons (indicated by red circle). Moreover, their inductive effect reduces electron density at the *ortho* carbons on the side aromatic amino groups on the main framework, which can suppress the overborylation.

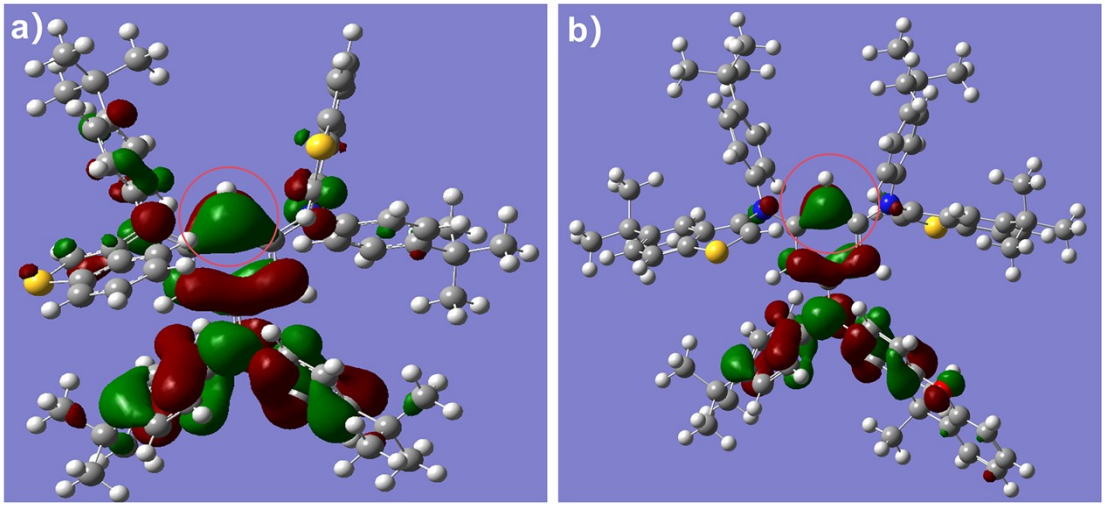

Figure S1. Distributions of highest occupied molecular orbital (HOMO) of (a) T-3, (b) X-3.

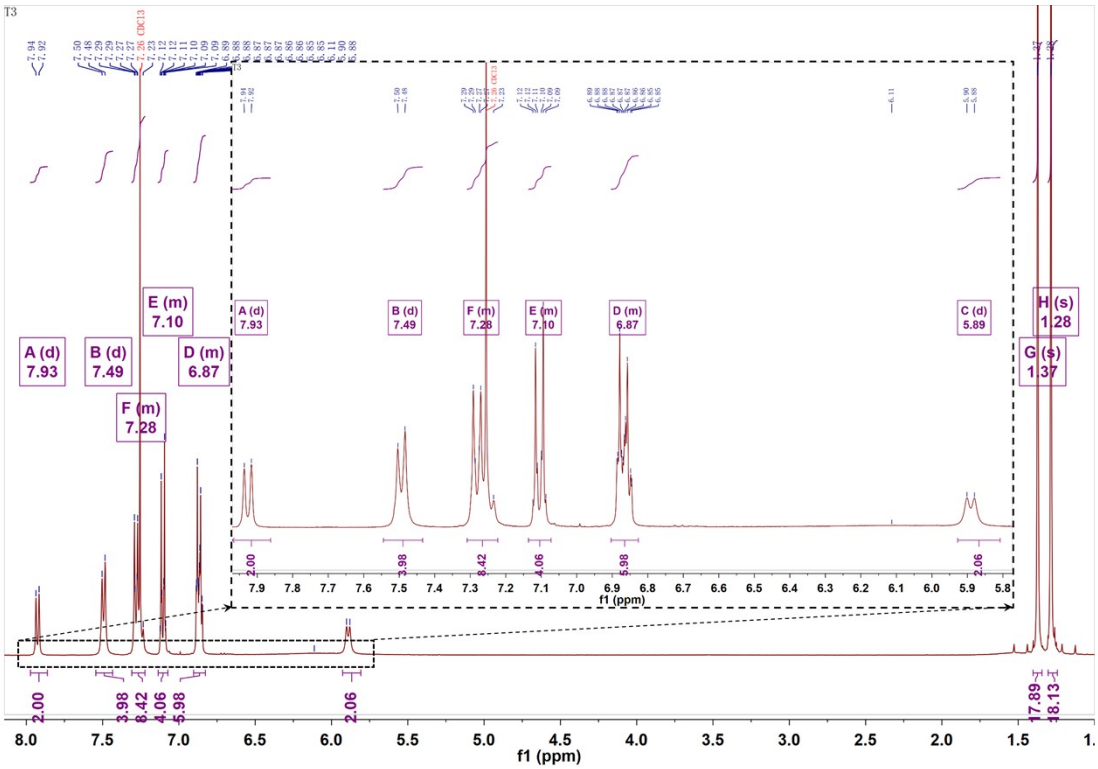

Figure S2. ^{1}H NMR spectrum of SBN-1 (400 MHz, $CDCl_3$).

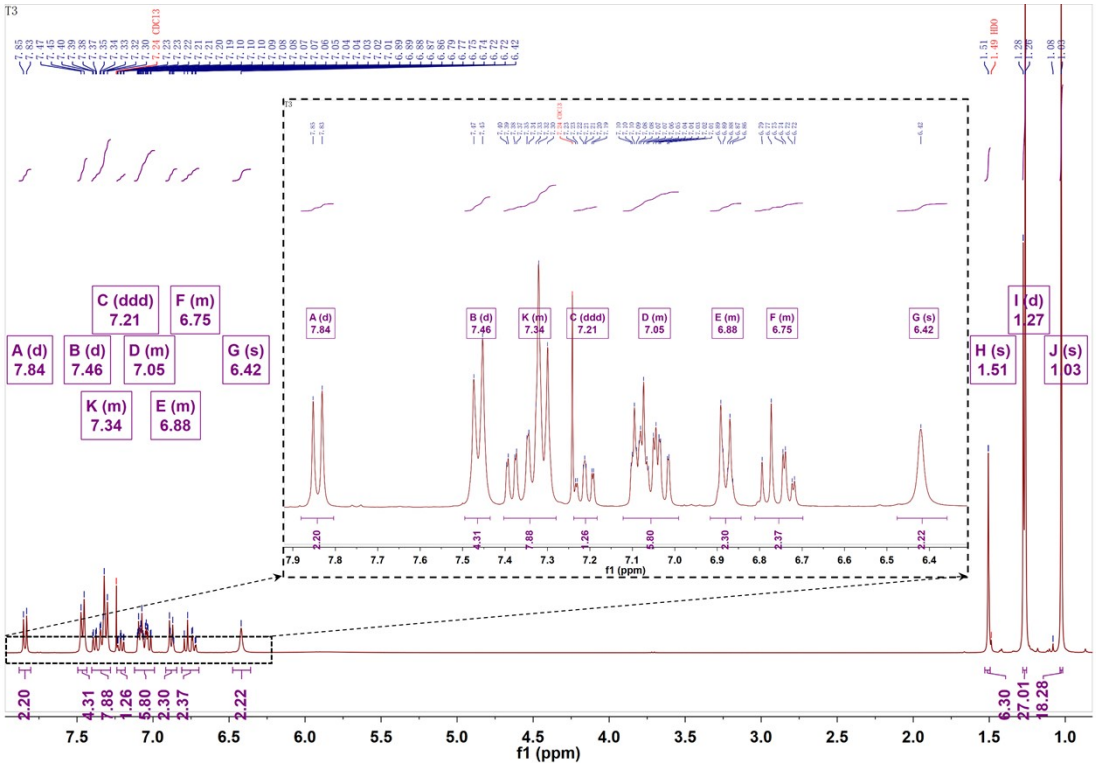

Figure S3. ^{1}H NMR spectrum of SBN-2 (400 MHz, $CDCl_3$).

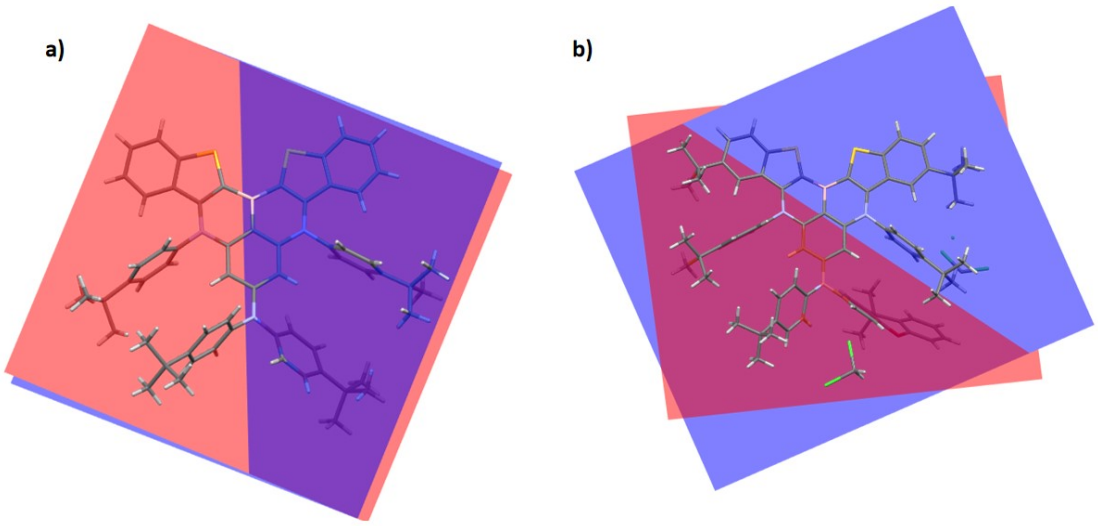

Figure S4. Crystal conformation and their dihedral angles of (a) SBN-1 and (b) SBN-2.

Table S1. Summary of TD-DFT calculation for DABNA-1, SBN-1 and SBN-2 at the S_0 and S_1 geometry at the b3lyp/6-31G(d,p) level.

Optimized structure	HOMO (eV)	LUMO (eV)	wavelength (nm)	Singlet energy (eV)	Triplet energy (eV)	Rate constants of fluorescence(k_F)
DABNA-1	-4.7538	-1.0925	428.60	2.8928	2.6376	5.05×10^{7}

SBN-1	-4.5029	-1.1406	466.42	2.6582	2.2787	7.32×10^7
SBN-2	-4.4730	-1.1061	467.30	2.6532	2.2817	8.38×10^7

Table S2. Correlation between FWHM and variation of ground state and excited state calculated at the b3lyp/6-31G(d,p) level.

Compound	FWHM [a](nm)	FWHM [b](nm)	ΔE [c](eV)	RMSD [d]
DABNA-1	26	28	0.2370	0.098
SBN-1	23	32	0.2582	0.237
SBN-2	18	22	0.2666	0.398

[a] Full width at half maximum (nm) of PL spectra in DCM solution at 298 K. [b] Full width at half maximum (nm) of EL spectra. [c] $\Delta E=E(S_1\leftarrow S_0)-E(S_1\leftarrow S_1)$ which represents the recombination energy from the excited state S_1 to the ground state S_0. [d] Root mean square displacement of optimized S_1 and S_0 structures, the formula is shown below.

$$RMSD=\sqrt{\frac{1}{N}\sum_{i}^{atom}\left[\left(xi-xi^{'}\right)^2+\left(yi-yi^{'}\right)^2+\left(zi-zi^{'}\right)^2\right]}$$

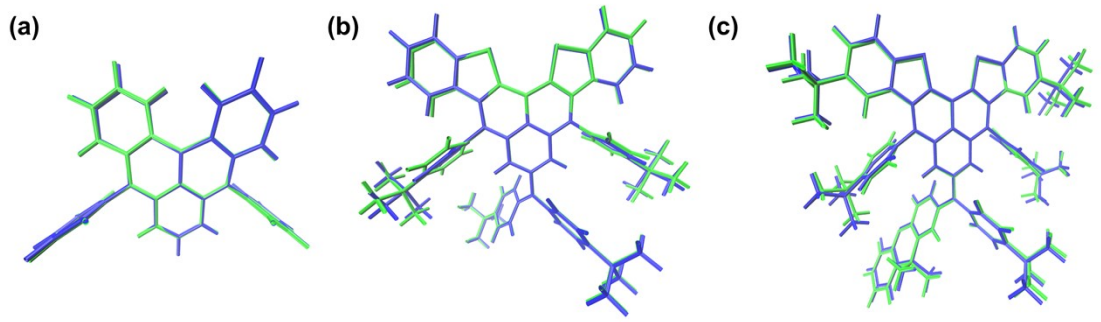

Figure S5. Comparison of the optimized structures of (a) DABNA-1, (b) SBN-1, (c) SBN-2 in the S_0 (blue) and S_1 (green) states.

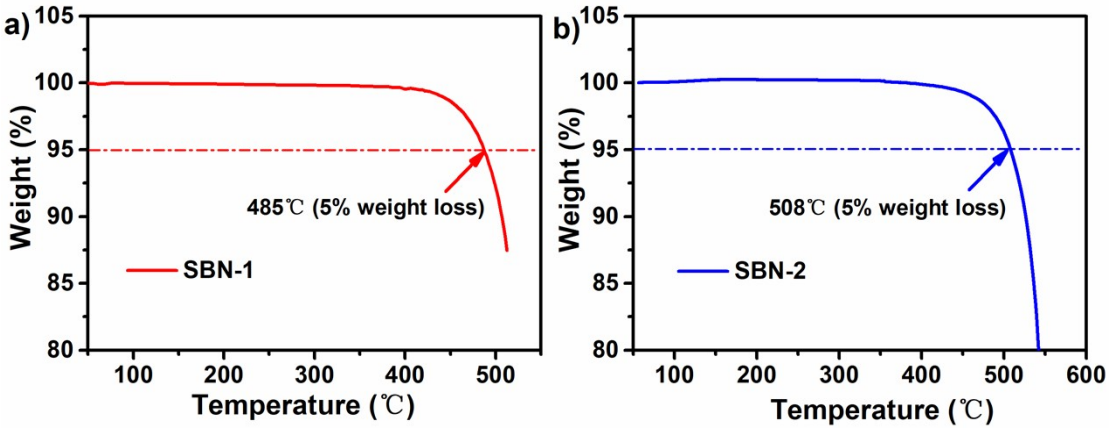

Figure S6. Decomposition temperature (T_d) of (a) SBN-1, (b) SBN-2.

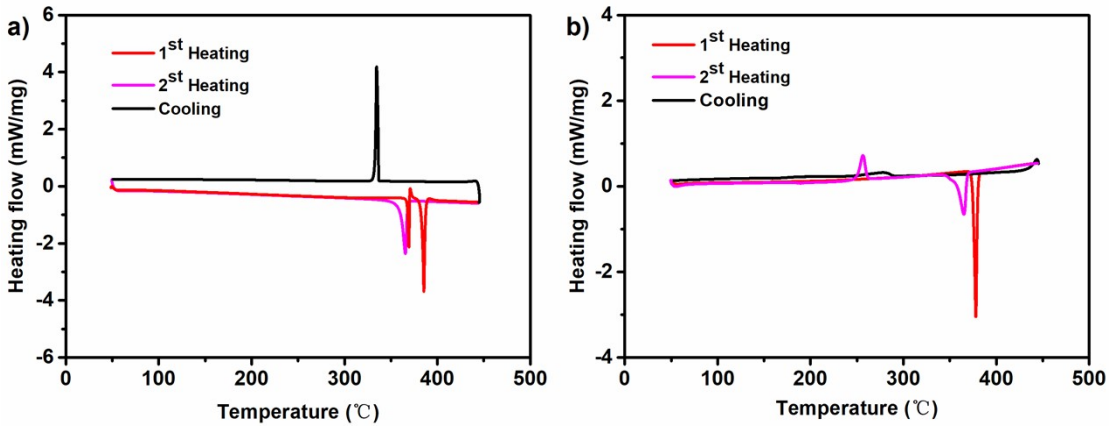

Figure S7. DSC curves of (a) SBN-1, (b) SBN-2.

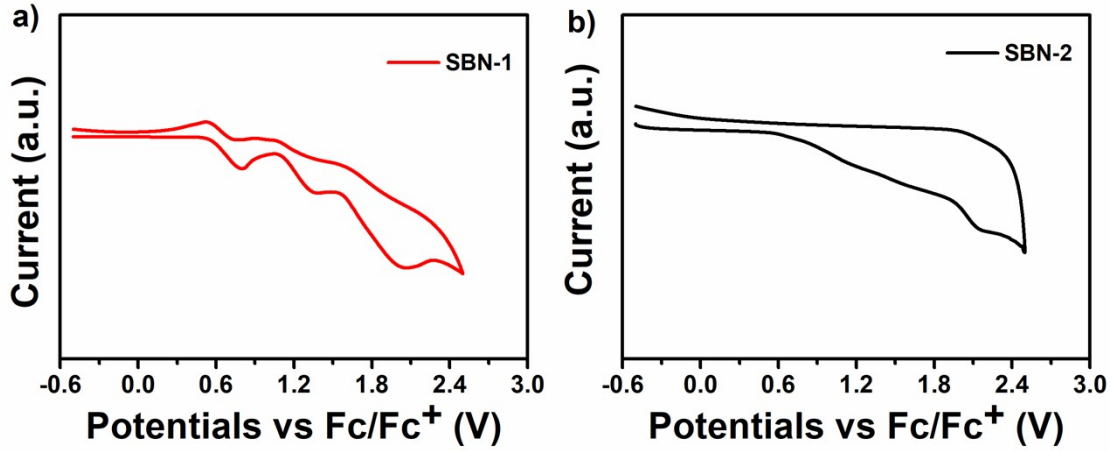

Figure S8. Cyclic voltammetry data for the oxidation of (a) SBN-1, (b) SBN-2.

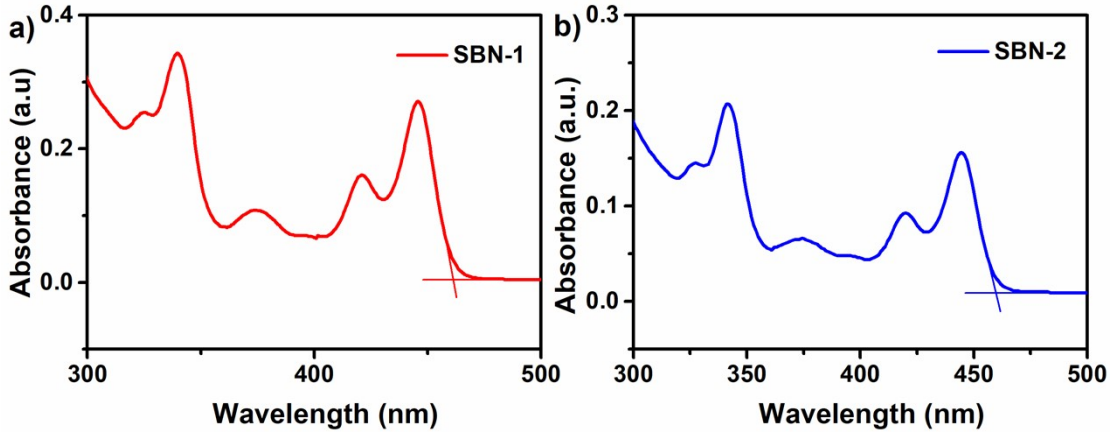

Figure S9. The absorbance (UV) spectra of (a) SBN-1, (b) SBN-2 and their absorption onsets in DCM solution.

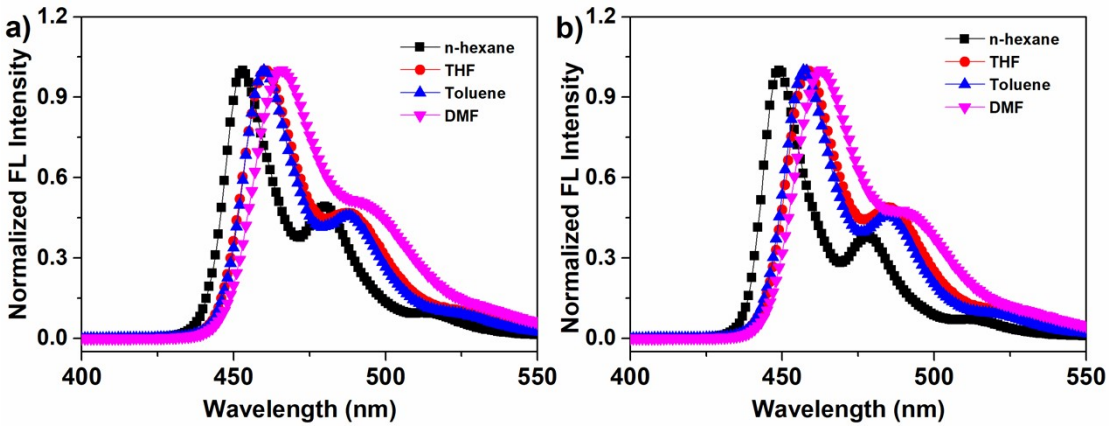

Figure S10. Normalized fluorescence spectra in different solvent (1×10^{-5} M) of (a) SBN-1, (b) SBN-2.

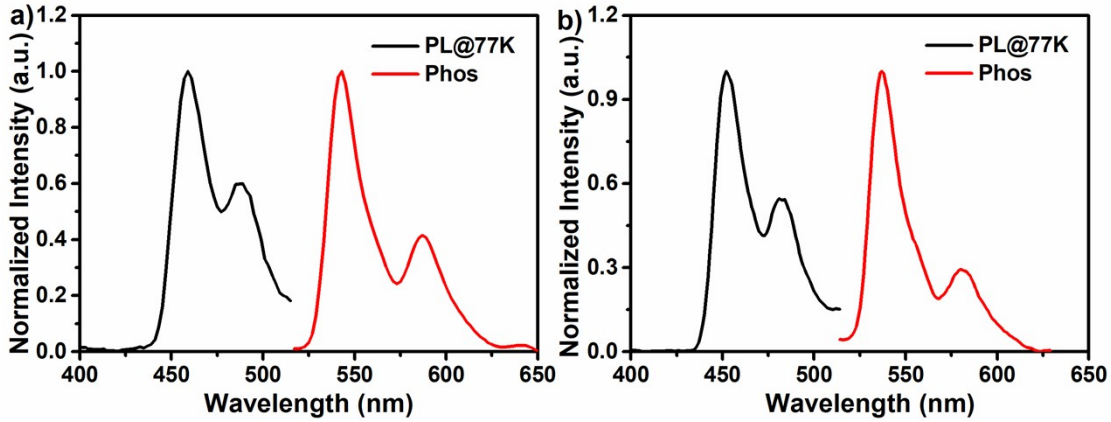

Figure S11. Normalized fluorescence and phosphorescence spectra in toluene solution (1×10^{-5} M, 77 K) of (a) SBN-1, (b) SBN-2.

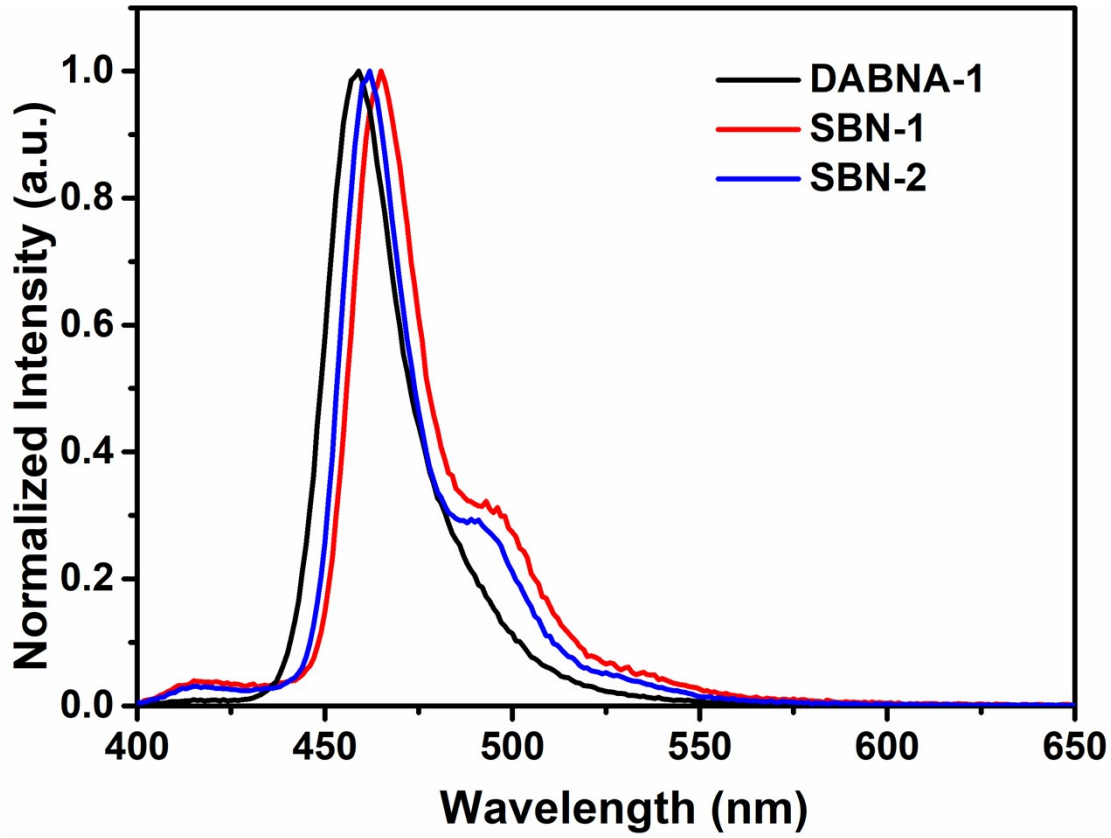

Figure S12. Normalized fluorescence spectra of 3 wt% of DABNA-1, SBN-1 and SBN-2 doped in FBH films.

Device Fabrication and Measurements

To fabricate the pure blue fluorescent OLEDs, the indium tin oxide (ITO) glass substrates with a sheet resistance of 15 Ω /sq a thickness and of 135 nm were cleaned in ultrasonic baths with optical detergent, deionized water, acetone and isopropanol successively. After dried in a convection oven at 120°C for 10 min, and ITO glass substrates were treated with plasma for 5 minutes. After transferring to substrates a vacuum chamber, the organic layers were deposited onto the ITO glass substrates with shadow mask at a rate of 1.0 Å s^{-1} under high vacuum (< 8 × 10^{-5} Pa). After depositing organic materials, Ag were successively evaporated at a rate of 5.0 Å s^{-1} through a shadow mask at a pressure of 5.0 × 10^{-4} Pa. A quartz crystal monitor was to monitor deposition rates. After depositing all layers, the OLED measurement modules were encapsulated using a capping glass in an evaporation chamber filled with O_2 and H_2O at a sparse concentration below 1 ppm. The getter was attached under the glass cap to absorb the residue moisture in the encapsulated device, which has an active

layer of 2 × 2 mm^2.

The EL spectrum, CIE coordinate and luminance intensity of the OLEDs were evaluated through Photo Research PR-670 at room temperature (298 K) in an air atmosphere. And the external quantum efficiency (EQE) was estimated in terms of brightness, electroluminescence spectrum and current density, according to assuming Lambertian distribution. The current−voltage−luminance (J−V−L) characteristics were recorded using a Keithley 2400 semiconductor characterization system and calibrating by a silicon photodiode. The lifetime was measured by using lifetime tester (Polaronix M6000). All measurements were carried out under argon conditions at room temperature.

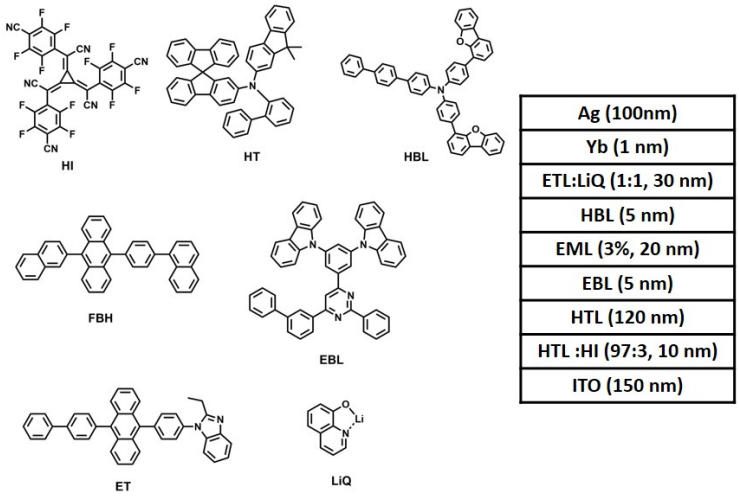

Figure S13. Molecular structures, and device structures and thickness of bottom device.

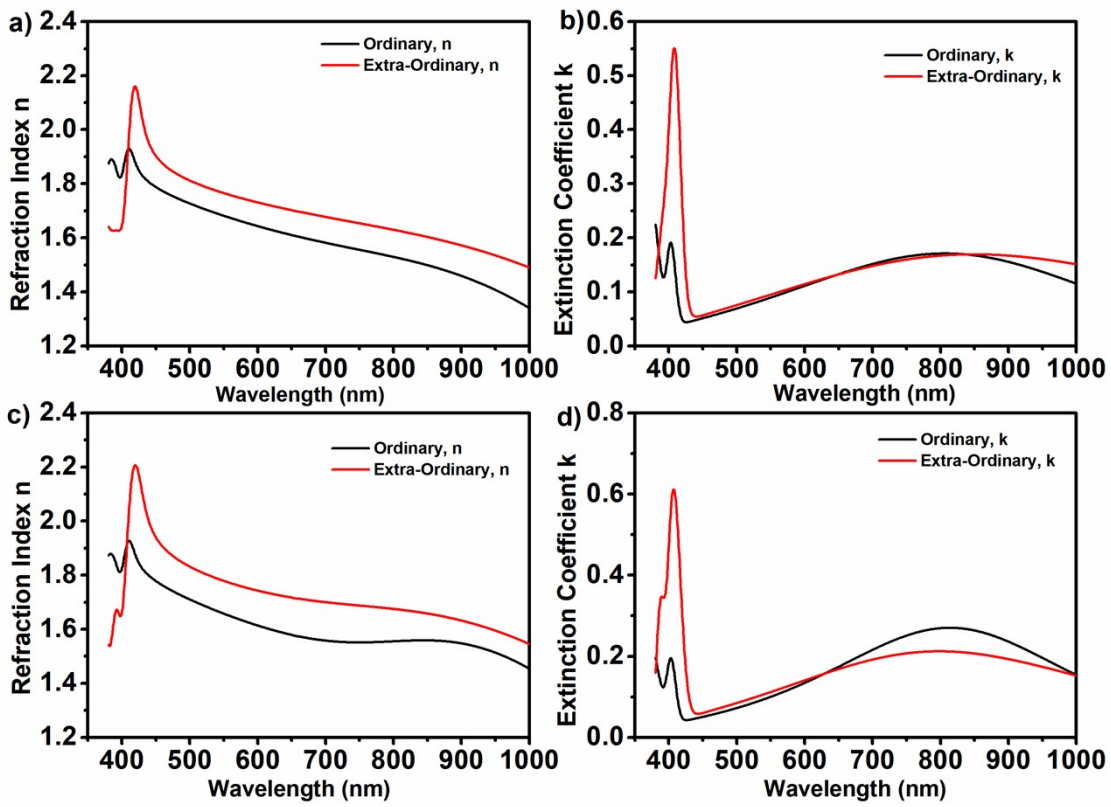

Figure S14. Ordinary (horizontal direction) and extraordinary (vertical direction) (a, c) refractive indices and (b, d) extinction coefficients of SBN-1 (a, b) and SBN-2 (c, d) doped films.

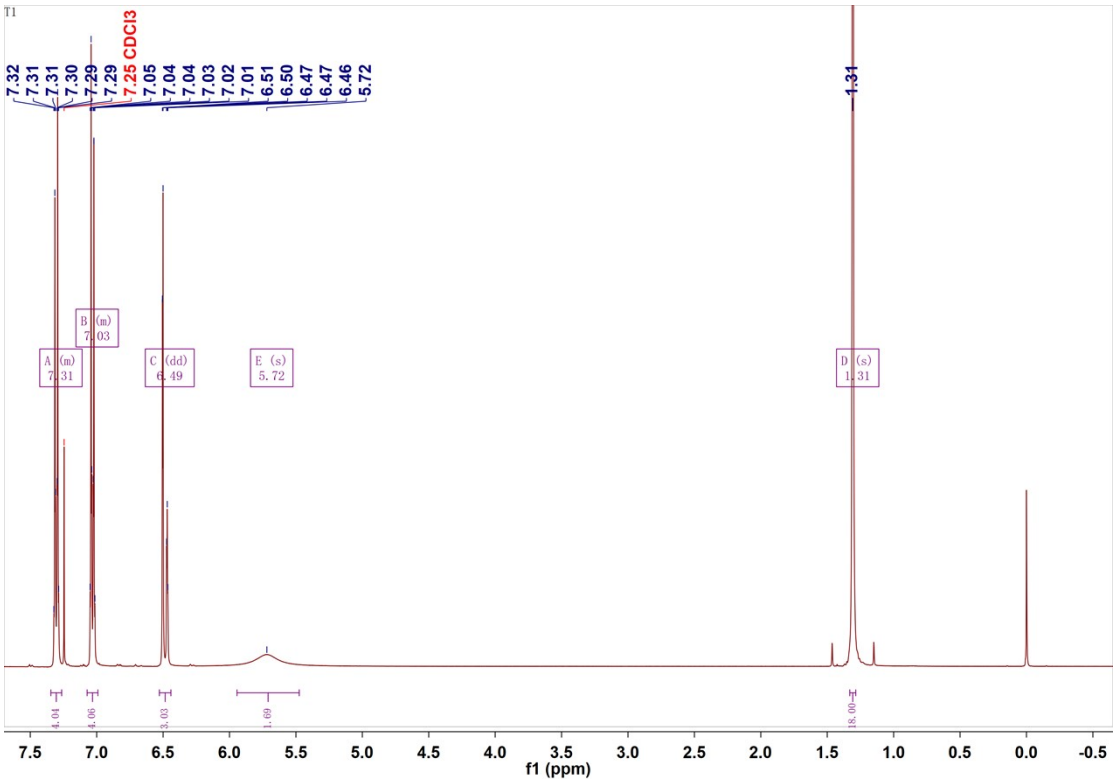

Figure S15. ^{1}H NMR spectrum of T-1 (400 MHz, $CDCl_3$).

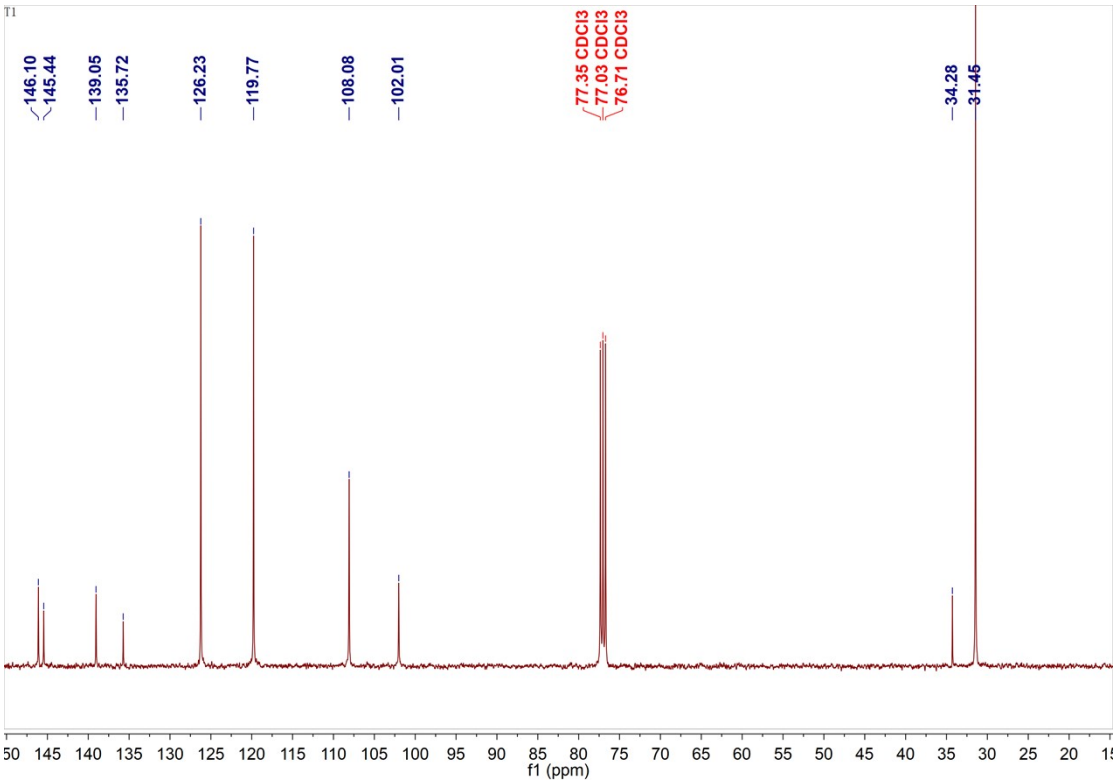

Figure S16. ^{13}C NMR spectrum of T-1 (101 MHz, $CDCl_3$).

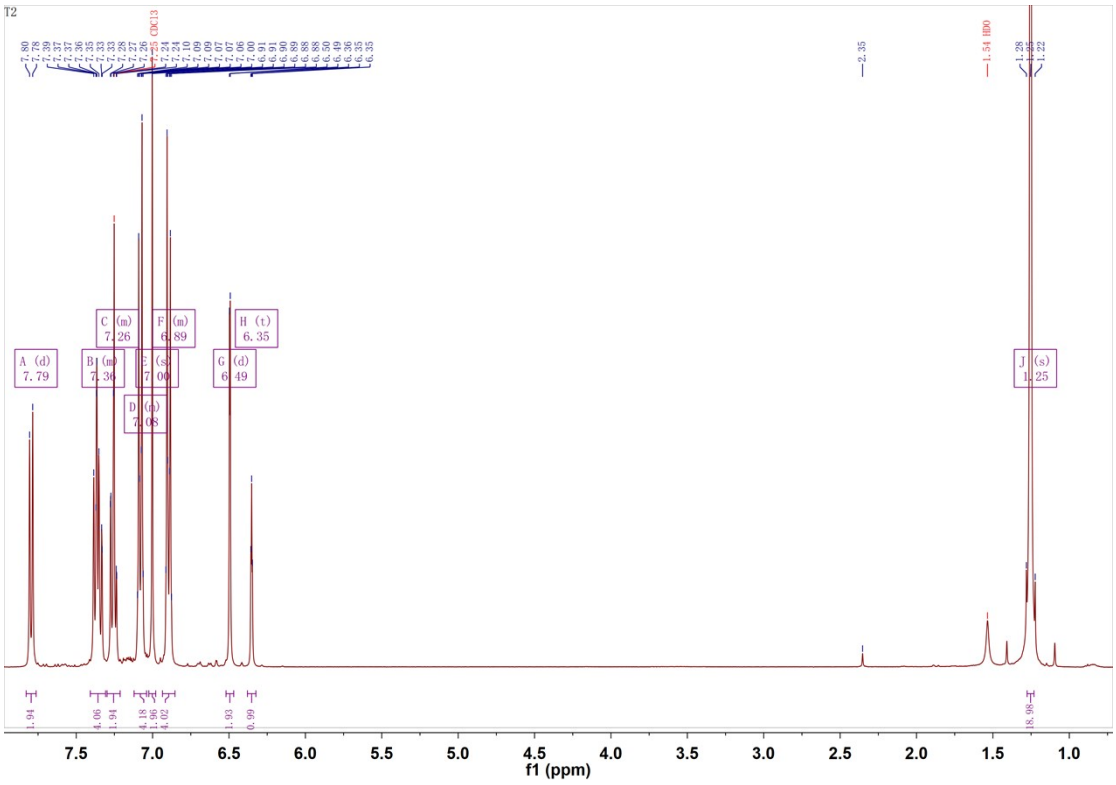

Figure S17. ^{1}H NMR spectrum of T-2 (400 MHz, $CDCl_3$).

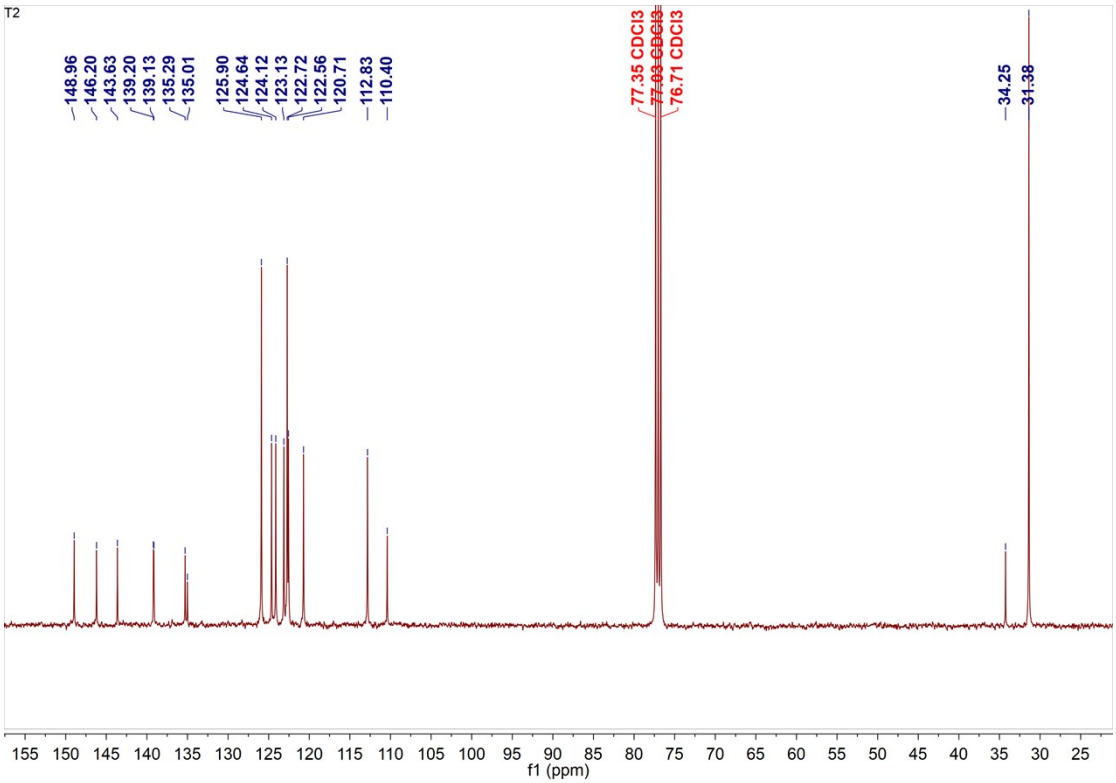

Figure S18. ^{13}C NMR spectrum of T-2 (101 MHz, $CDCl_3$).

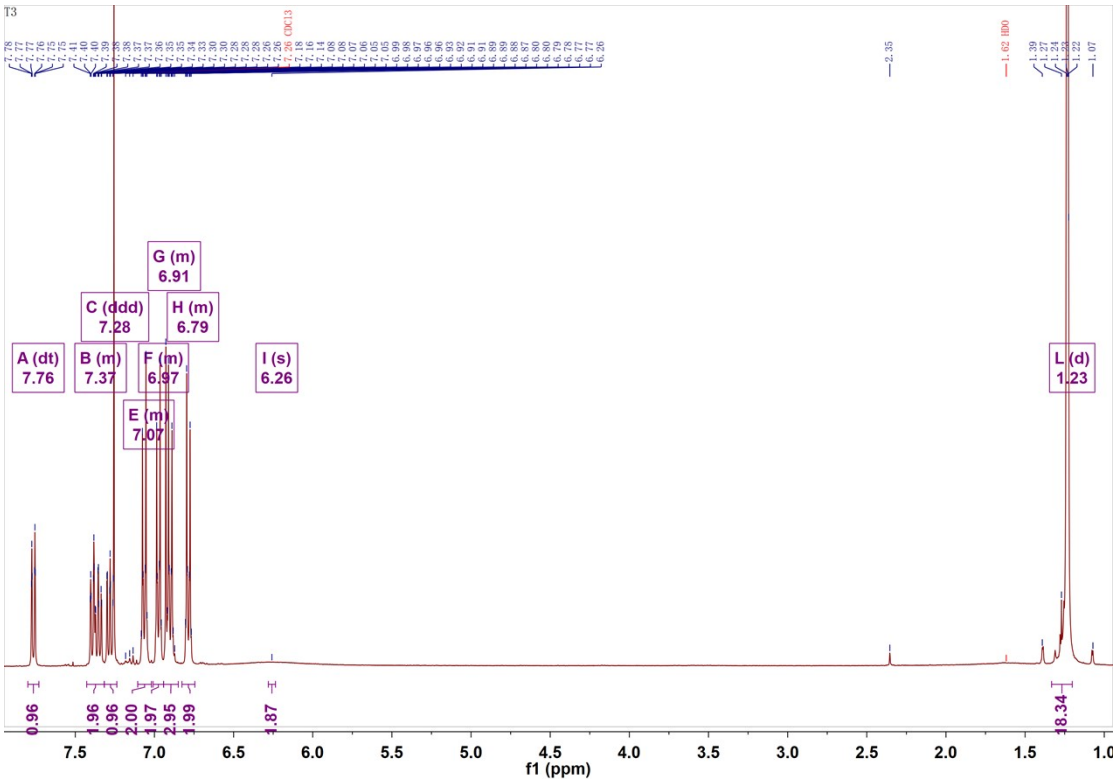

Figure S19. ^{1}H NMR spectrum of T-3 (400 MHz, $CDCl_3$).

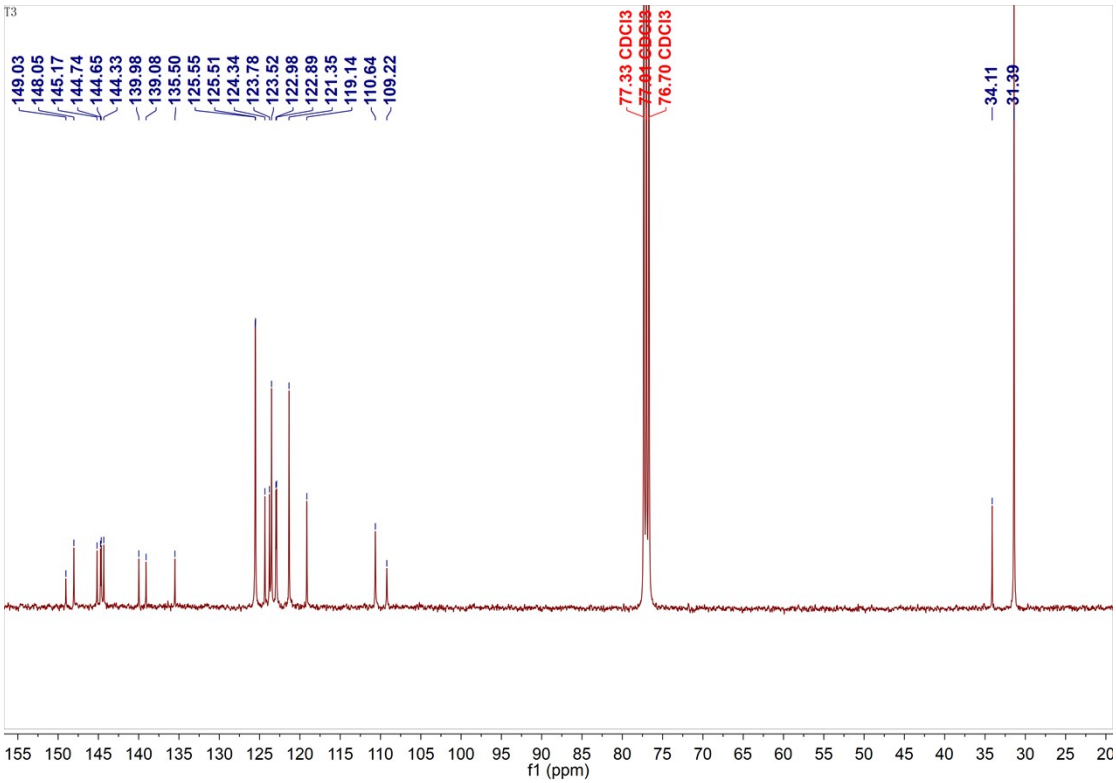

Figure S20. ^{13}C NMR spectrum of T-3 (101 MHz, $CDCl_3$).

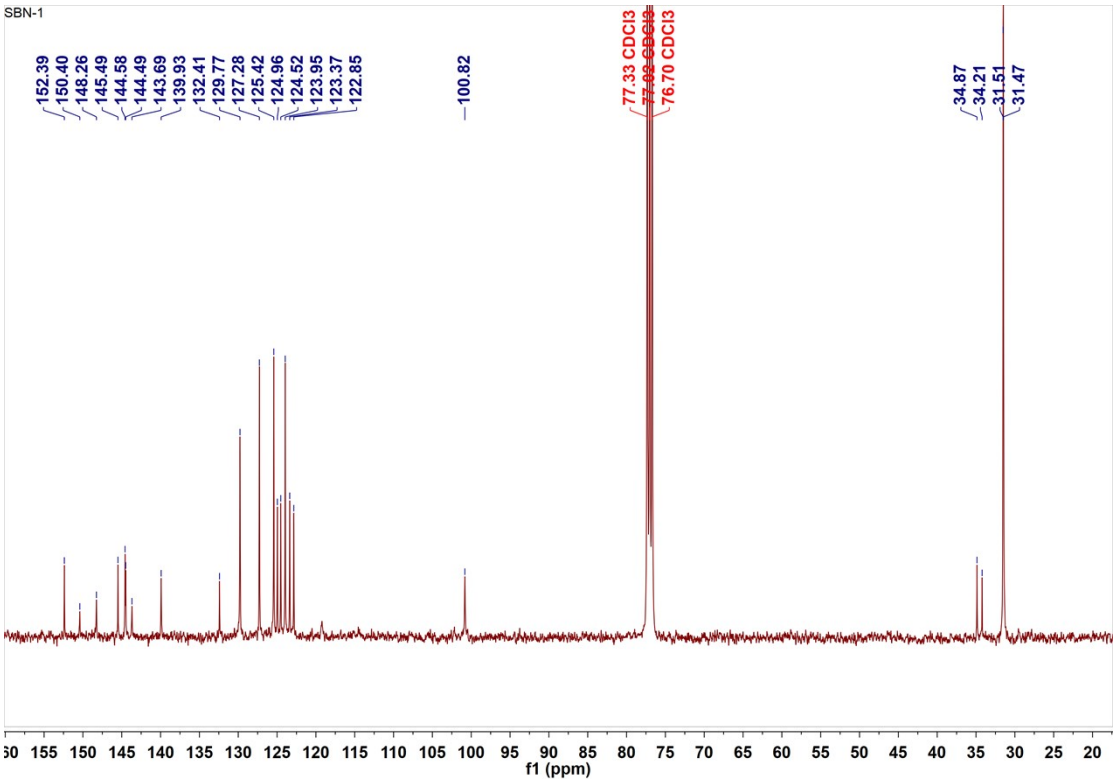

Figure S21. ^{13}C NMR spectrum of SBN-1 (101 MHz, $CDCl_3$).

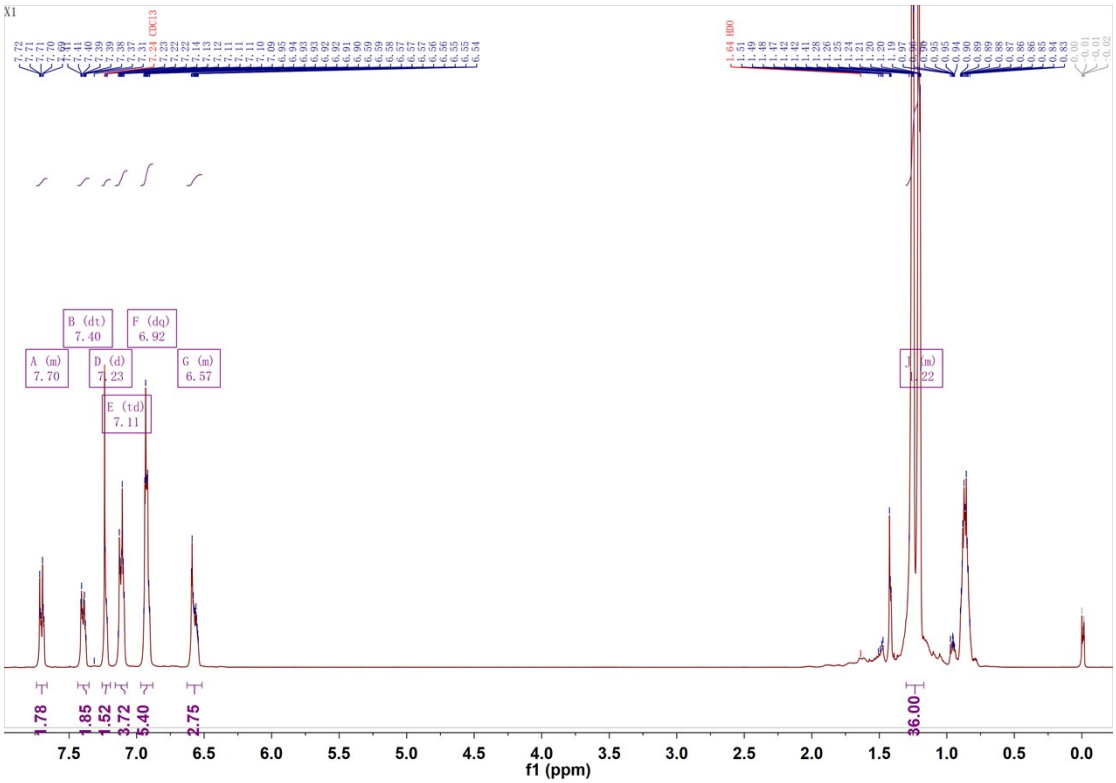

Figure S22. ^{1}H NMR spectrum of X-1 (400 MHz, $CDCl_3$).

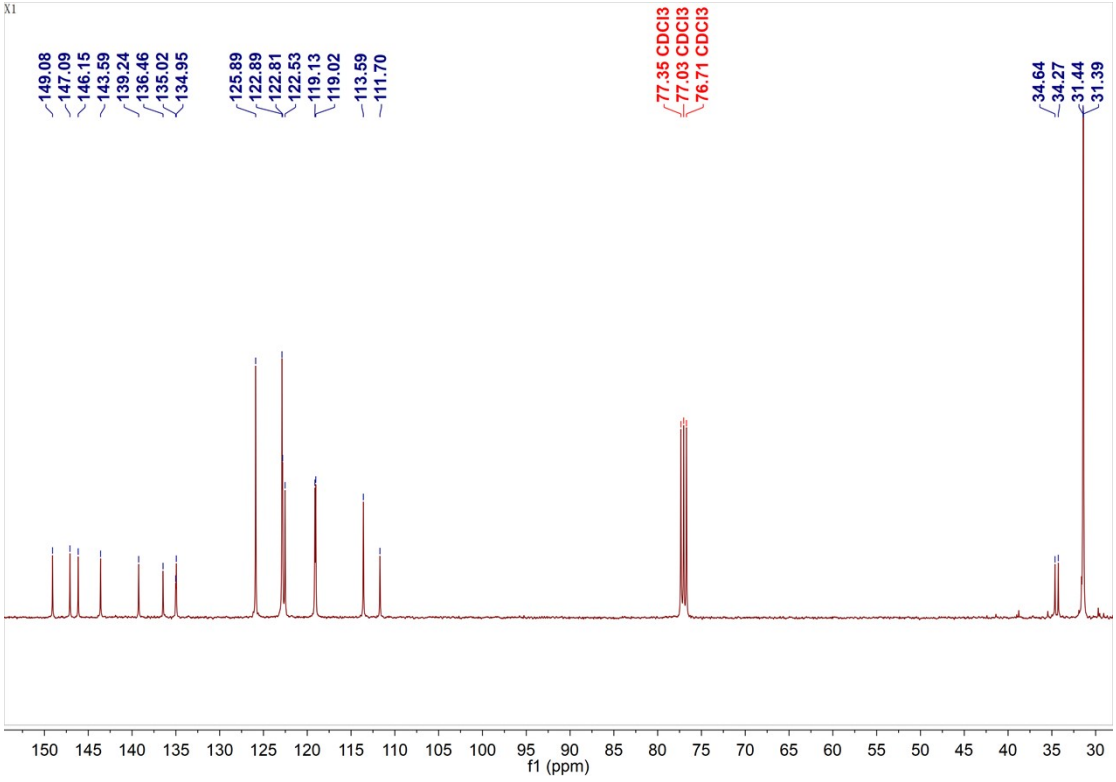

Figure S23. ^{13}C NMR spectrum of X-1 (101 MHz, $CDCl_3$).

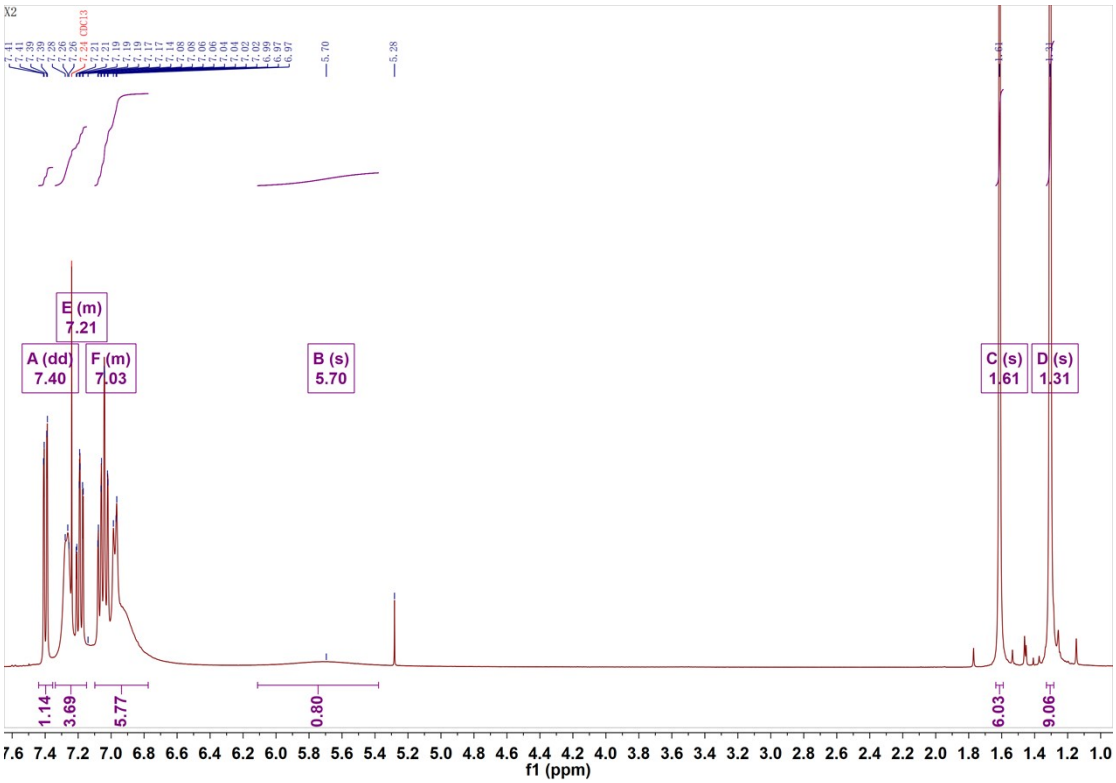

Figure S24. ^{1}H NMR spectrum of X-2 (400 MHz, $CDCl_3$).

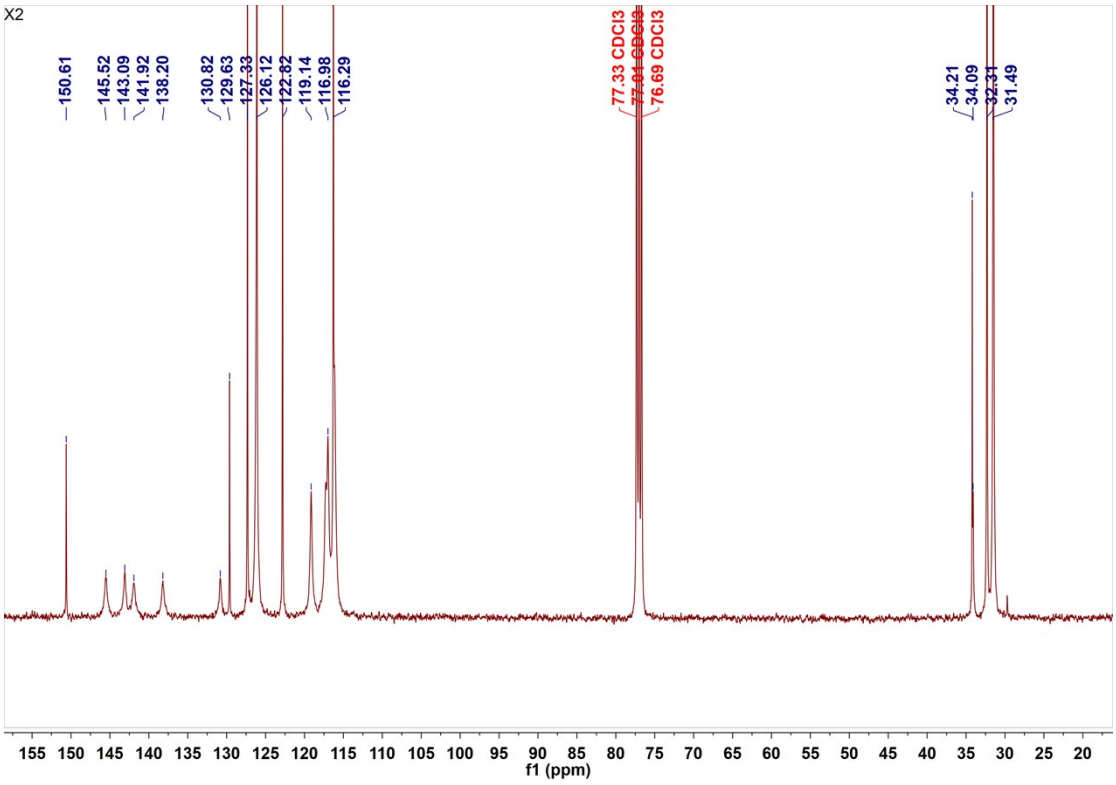

Figure S25. ^{13}C NMR spectrum of X-2 (101 MHz, $CDCl_3$).

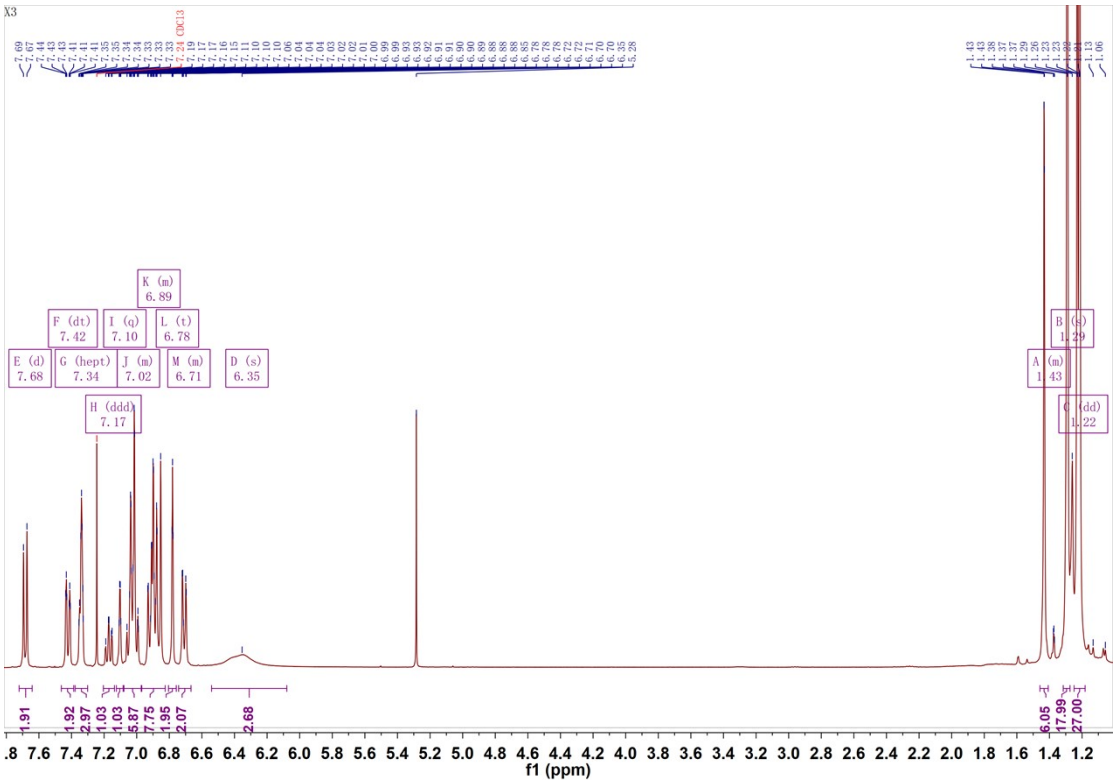

Figure S26.[1]H NMR spectrum of X-3 (400 MHz, $CDCl_3$).

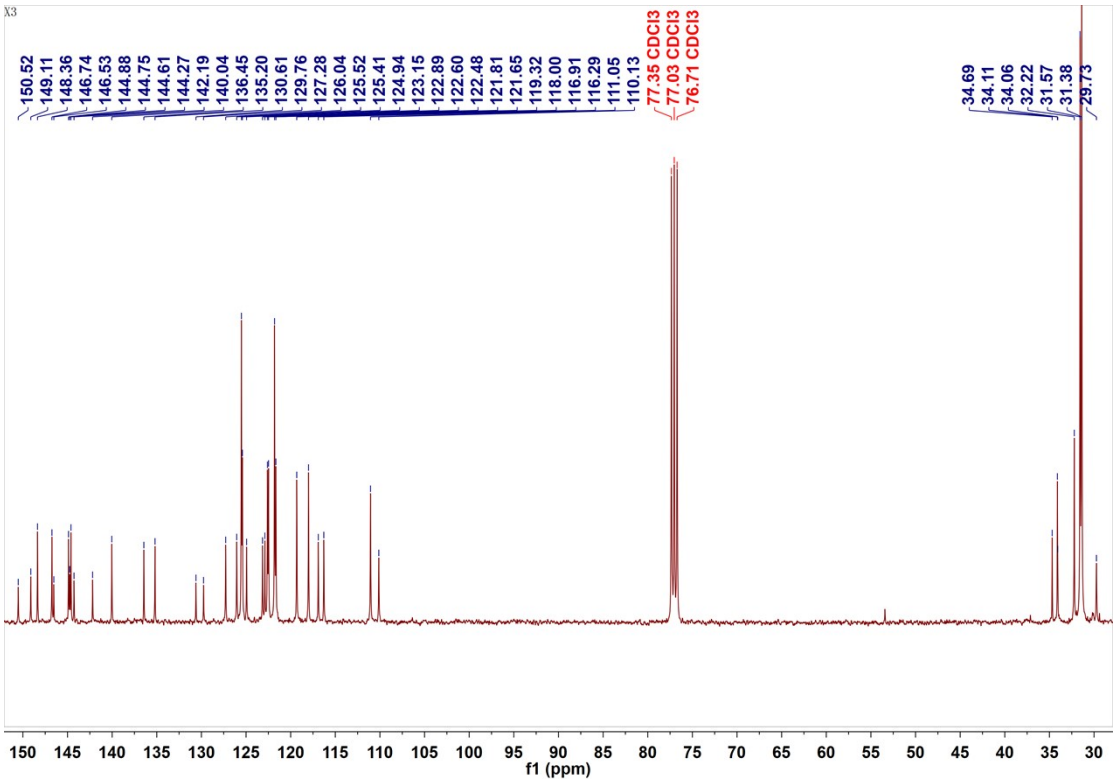

Figure S27. [13]C NMR spectrum of X-3 (101 MHz, $CDCl_3$).

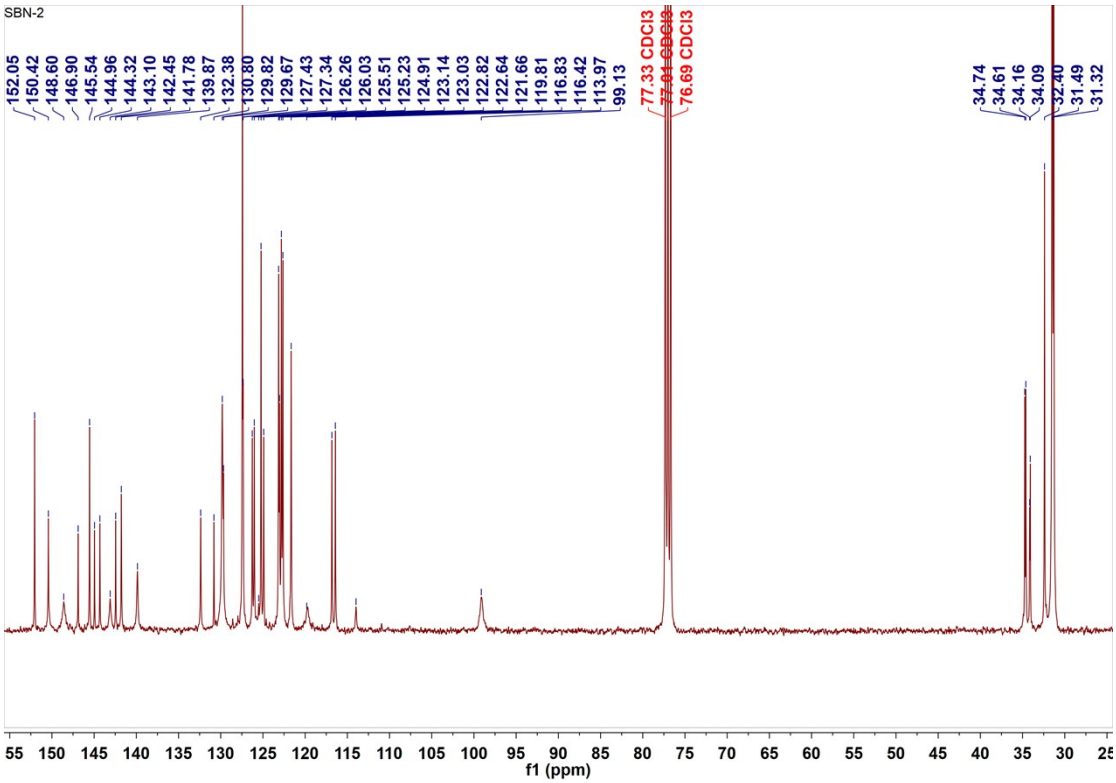

Figure S28. ^{13}C NMR spectrum of SBN-2 (101 MHz, $CDCl_3$).

1. I. Kim, K. H. Cho, S. O. Jeon, W.-J. Son, D. Kim, Y. M. Rhee, I. Jang, H. Choi and D. S. Kim, *JACS Au*, 2021, **1**, 987-997.